THE ASTROPHYSICAL JOURNAL, 347:627–639, 1989 December 15

ABSORPTION LINES AT $z > 2.3$ IN SPECTRA OF QUASI-STELLAR OBJECTS

PUSHPA KHARE[1] AND DONALD G. YORK[2,3]
University of Chicago
AND
RICHARD GREEN[3]
Kitt Peak National Observatory
Received 1988 June 20; accepted 1989 June 8

ABSTRACT

A magnitude-limited sample of nine QSOs with redshifts $z \gtrsim 3$ was selected to look for intervening absorbers with $z \sim 2.3$–3.0. Thirty-five possible systems are found, 22 of which were not previously known. Our main purpose was to search for a change in the number of the absorbers with redshift. A simple power law [$dM/dz \propto (1+z)^{\gamma}$, $\gamma = 0.5$–1 for no evolution] does not fit the data, owing to an excess of absorbers at $z = 2$ to 2.5. In an equivalent path length $\Delta z \simeq 1.0$ at $z = 2.4$, four intervening absorbers are found, whereas in $\Delta z \simeq 1$ at $z \sim 3.2$, no intervening absorbers are found. In addition, we find a slight lowering of ionization with z, and an increase in the relative number of weak C IV systems is found as z increases. All of these results must be confirmed in larger samples.

Subject headings: galaxies: intergalactic medium — quasars

I. INTRODUCTION

It is generally accepted that the narrow, heavy-element absorption-line systems in the spectra of QSOs are produced by galaxies along the line of sight to these QSOs. A study of these lines promises to offer unique information about galaxies in the remote past, particularly about the change with redshift of the physical properties of the absorbers: space density, radius, ionization level, and element abundances. The study of absorption systems can therefore offer important clues about the epoch of galaxy formation. Statistical studies of the evolution of heavy-element absorption systems have been undertaken by several authors (Khare-Joshi and Perry 1981; Bergeron and Boisse 1984; Foltz *et al.* 1986; Lanzetta, Turnshek, and Wolf 1987; Caulet 1989; and references therein). These authors have used the absorption systems defined by the C IV doublets, which form the majority of the known absorption systems, and/or Mg II doublets. The absorption systems with a relative velocity larger than a few thousand kilometers per second, compared to the background QSO, appear to have an exponential distribution in rest equivalent width. Highly ionized species, e.g., C IV and Si IV, appear more often than first ions (Mg II, Si II, etc.). Most important, the absorption cross sections of galaxies appear to be evolving, the cross section having been higher in the past (Bergeron 1988). The studies so far have been confined to absorption redshifts smaller than ~ 2. The data sets are small, the statistical uncertainties are large, and the results are also consistent with no evolution in the properties of the absorbers. It is, therefore, highly desirable that the data sets be enlarged to reduce the statistical errors and that they be extended to higher absorption redshifts to provide greater discernment on the question of evolution.

In this paper, we present moderate-resolution observations of nine QSOs in the redshift range of 2.99–3.41. The observations cover the regions between Lyα and C IV emission lines, usually from 5200–6600 Å. Thirty five systems are found, 22 of which were not previously known. For a statistical sample of systems detected at the 5 σ level, 16 C IV systems are found, covering a redshift range of 2.36–3.22. The details of observations and data reduction are presented in § II. The properties of the absorption systems are discussed in § III, where we extend the redshift range to lower z by including the homogeneous, unbiased sample of Foltz *et al.* 1986 (hereafter FWPSMC) to study the evolution of the cross section of absorbers. The results are summarized in § IV.

II. OBSERVATIONS AND DATA REDUCTION

Targets were selected by choosing all QSOs in the catalog of Hewitt and Burbidge (1987) with visual magnitude, V, less than 18.8 and redshift, z, greater than 3.0 (rounded to the nearest tenth). The subsets of this sample between right ascension (R.A.) 21^h and 8^h (increasing R.A.) and north of declination $-10°$ were our prime targets for October observing with the Mayall 4 m telescope at Kitt Peak National Observatory. Observing as close to the meridian as possible, we chose the brightest of the 16 candidates. The observing constraints left four candidates brighter than 18.8 unobserved: Q 0216+080, $z = 2.99$, $V = 18.1$; Q 0029+073, $z = 3.27$, $V = 18.4$; Q 0301−005, $z = 3.3$, $V = 18.5$; and Q 0045−036, $z = 3.14$, $V = 18.6$. Of four objects with $V = 18.8$: Q 2233+131, $z = 3.28$; Q 2359+068, $z = 3.25$; Q 0143−0.15, $z = 3.14$; and Q 0153+045, $z = 2.99$, only the last was observed. Of course, the variability range of these objects is not known, so strict definition of a magnitude-limited sample below 18.0 is not possible. For all objects, the candidates can be regarded as randomly selected, without regard to known absorption-line features. Table 1*a* lists the objects observed, along with their emission redshifts, visual magnitude, and the absorption systems previously observed in their spectra, as noted by Hewitt and Burbidge (1986).

[1] Visiting scholar, on leave of absence from the Physics Department, Utkal University, Bhubaneswar, India.
[2] Enrico Fermi Institute, Department of Astronomy and Astrophysics.
[3] Guest observers on the 4 m Mayall Telescope, Kitt Peak National Observatory, operated for the National Science Foundation by the Associated Universities for Research in Astronomy.

TABLE 1A

JOURNAL OF OBSERVATION[a]

QSO	1950 Coordinates	z_{em}	V	Known z_{abs}
0014+81	0:14:4.10	3.41	16.5	3.32
(S5)	81:18:28.4			1.11
0114−089	1:14:52.8	3.16	17.4	...
(UM 670)	−8:56:56			
0120+026	1:20:21.3	3.272	18.0	...
(UM 100)	2:41:53			
0153+045	1:53:59.7	2.99	18.8	...
(UM 148)	4:30:58			
0302−003	3:2:16.3	3.285	18.37	...
	−0:19:47			
0642+449	6:42:53.02	3.402	18.49	3.343
(OH 471)	44:54:31.1			3.246
				3.191
				3.122
				2.971
				2.911
				2.491
				2.447
				2.015
				0.805
0731+653	7:31:34.3	3.035	18.5	...
	65:19:50			
PKS 2126−158	21:26:26.69	3.27	17.3	2.7685
	−15:51:51.5			2.6381
				2.3938
2348−011	23:48:24	3.01	18.0	2.598
(UM 184)	−1:8:42			

[a] Data from Hewitt and Burbidge 1986.

TABLE 1B

JOURNAL OF OBSERVATION

QSO	GMT (hr, min)	Hour Angle (hr, min)	Exposure Time (s)
0014+81	4:20	1:43E	900[a]
	4:36	1:26	900[a]
	2:50	3:08	900[b]
	3:07	2:52	900[b]
	3:32	2:23	1300[c]
	3:28	2:22E	1300[c]
0114−089	8:06	1:04W	1500[a]
	8:37	1:35W	600[a]
	5:59	0:59E	2000[b]
	6:34	0:24E	2000[b]
	7:49	0:56W	3000[c]
	6:26	0:24E	3200[d]
0120+026	5:58	1:11	2000[a]
	6:33	0:35	4000[a]
	4:47	2:17	2500[b]
	5:32	1:32	1200[b]
	4:51	2:09	2000[c]
	5:27	1:33	2000[c]
	4:02	3:01	2400[d]
	4:44	2:13E	2400[d]
0153+045	8:55	1:15W	1200[a]
	9:18	1:37W	1200[a]
	7:26	0:11E	3600[b]
	8:48	1:15W	3500[c]
0302−003	9:51	1:01W	3500[a]
	8:34	0:12E	1800[b]
	9:06	0:20W	1800[b]
	10:00	1:19W	2500[c]
	7:50	0:48E	3600[d]
0642+449	11:04	1:26	2500[a]
	9:46	2:41	2000[b]
	10:23	2:04	2000[b]
	10:58	1:28	2000[b]
	11:02	1:20	2400[c]
	11:43	0:39	2400[c]
	9:02	3:17	3900[d]
	10:08	2:11	3900[d]
	11:14	1:04	3900[d]
0731+653	11:58	1:22	1800[a]
	11:40	1:36	2500[b]
2126−158	3:13	0:01E	1500[a]
	3:41	0:27W	1500[a]
	2:13	0:58E	1500[b]
	2:46	0:21	2000[c]
	2:34	0:29	2500[d]
2348−011	5:08	0:28	2000[a]
	3:32	2:01	4000[b]
	4:07	1:21	2000[c]

[a] Observed on 1987 Oct 17 from 5200 to 5550 Å.
[b] Observed on 1987 Oct 18 from 5550 to 5900 Å.
[c] Observed on 1987 Oct 19 from 5900 to 6250 Å.
[d] Observed on 1987 Oct 20 from 6250 to 6600 Å.

The observations were made with the Ritchey-Chrétien (RC) spectrograph on the nights of 1987 October 17–20. The grating used was the 632 l mm^{-1} grating in second order with a 1".5 slit, giving a nominal resolution of 1.4 Å in 3.4 pixels of the Texas Instrument 800 × 800 CCD. The grating was set at one position for each night, and all objects were observed each night when possible. Thus, we gradually built up the spectrum from 5200 to 6600 Å. This region was chosen to sample the region 1216 Å–1550 Å in the rest frame of a QSO with an emission redshift of 3.3, slightly above the mean redshift of our observed sample ($\bar{z} = 3.2$, Table 1A). This region is chosen to pick up lower redshift doublets of C IV ($\lambda_{rest} \sim 1550$), while avoiding the confusing region of the Lyα forest ($\lambda_{rest} < 1216$), where identifications are uncertain. Of course, for objects at $z_{em} > 3.3$, part of the Lyα forest was observed, and for objects at $z < 3.3$, the longest wavelengths observed fall beyond any expected C IV doublets from intervening gas clouds. The GMT, hour angle date, and duration of each observation is given in Table 1B.

The image processing was done by using IRAF reduction packages. The one-dimensional spectrum was extracted using profile weighting perpendicular to the dispersion, the peak of the weighting function following the ridge of image intensity. A background value for each wavelength was derived by interpolation in a smooth function fit to the sky from either side of the stellar image; that value was then subtracted to produce the net object spectrum. Reference He-Ne-Ar lamp spectra were recorded in separate frames along with each object exposure. No shifts greater than 1/10 of a pixel were found between successive exposures of the same wavelength region on a given object. Parts of spectra which were observed more than once were added together pixel by pixel. The resultant spectra were then calibrated by using the average of the He-Ne-Ar spectra taken before and after the individual QSO observations.

The resultant spectra are shown in Figure 1. The ~300 Å regions observed on different nights are presented separately in four blocks for each spectrum. In Figure 1, we have scaled and combined these so that the different portions match smoothly with the neighboring regions. This presentation procedure distorts the apparent signal-to-noise (S/N) ratio which is enhanced or reduced artificially due to the scaling. For analysis

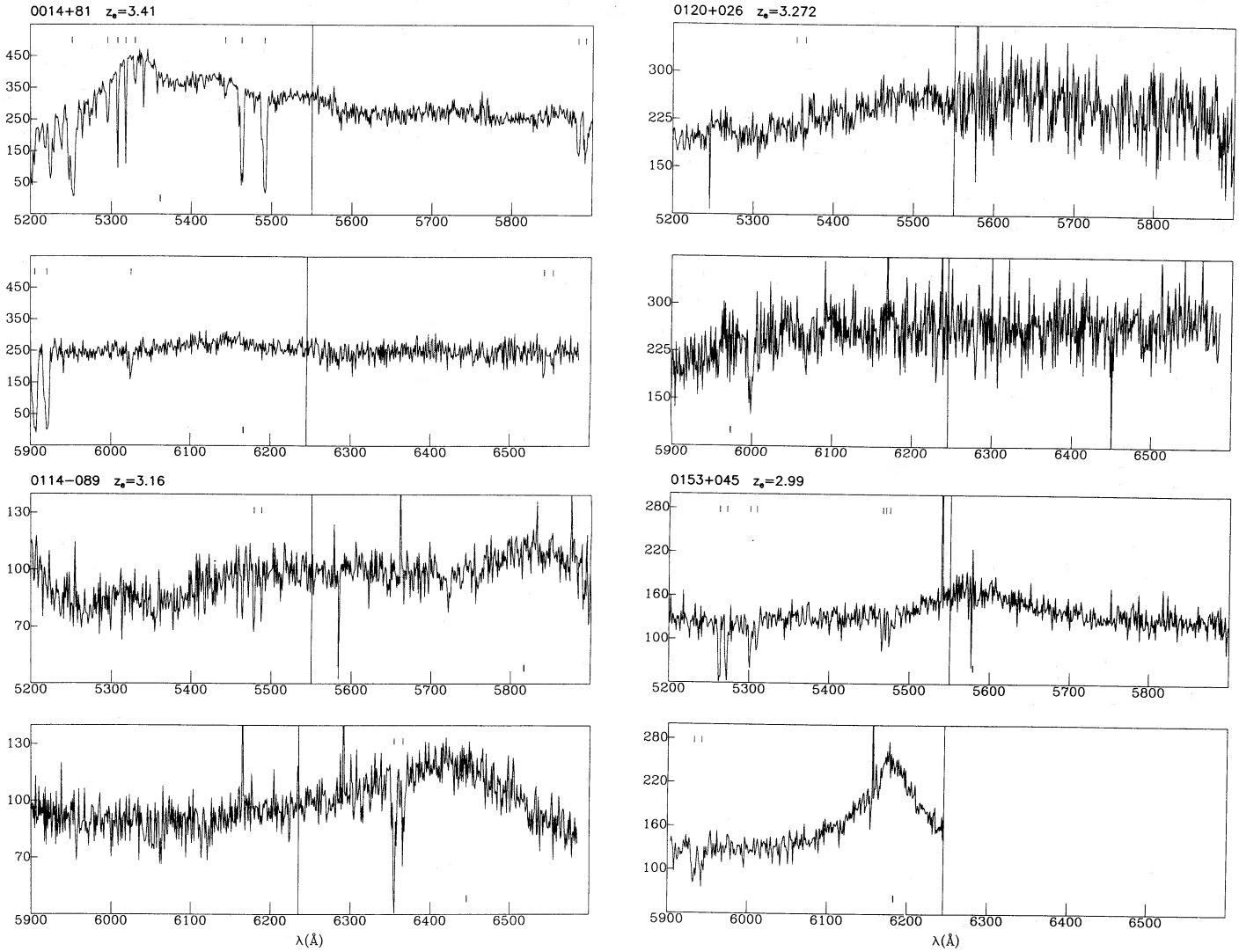

FIG. 1.—Reduced spectra of nine high-redshift QSOs at sampling intervals of 2 Å. Labels at the top indicate the *identified* lines in Table 1 (5 σ). Tick marks below the spectra indicate the position of emission lines at the emission-line redshift tabulated in Table 1. If only one tick exists, it is for Si IV. If two ticks exist, with one on the left end of the top panel, the tick marks label Lyα, Si IV. Otherwise, they label Si IV ($\lambda\lambda$1393, 1402) and C IV.

purposes, each portion of each spectrum was analyzed separately, taking the measured S/N ratio into account.

We search for telluric lines in the spectra of standard stars, spectra of which were taken along with those of the QSOs. No strong lines were found in the QSO spectra above the 2 σ level of significance. The S/N ratio was determined for the line-free regions of each of the spectra, and the average was taken over regions where the signal did not change by more than 25%, but always over $\lesssim$300 Å. (This approach gives a true S/N from all noise sources—preflashing, readnoise, weak absorption lines, and photon noise from the source—and is more exact than assuming that pure photon statistics dominate). In some cases, especially around the Lyα emission line, the S/N ratio could not be determined because of the lack of line-free regions. In such cases, the S/N ratio was taken to be the same as that for the neighboring region of the spectrum, unless the signal differed by more than a factor of 2, in which case S/N was appropriately scaled. S/N ratio varied from 4.62 to 26.82; however, for 60% of the spectra, the S/N ratio was larger than 10. In any case, the S/N ratio was sufficient to detect C IV doublets with each line having a rest equivalent width of $\gtrsim$300 m Å, 5 σ.

To identify the absorption lines, a line list was compiled by picking lines with observed equivalent width larger than 5 σ when σ (Å) was calculated according to the formula

$$\sigma(\text{Å}) = \Delta\lambda\sqrt{n}/(\text{S/N}) ,$$

where $\Delta\lambda$ is the pixel size in angstroms, n is the width of continuum searched for absorption in number of pixels, and S/N is the signal-to-noise ratio.[4]

[4] The equivalent width of a single pixel feature is simply the count rate in that pixel times the width of the pixel, $\Delta\lambda$, divided by the continuum count rate. A false feature caused by noise of N counts s^{-1} thus produces a false W_λ equal to $\Delta\lambda N/S$, where S is the continuum count rate, or $W = \Delta\lambda/(\text{S/N})$. If more than one pixel is used to make a measurement, the expected equivalent width error is smaller because more photons are used in the measurement, but the gain is only quadratic in number of pixels for a photon-limited detection system. On the other hand, the total wavelength range is large, so the uncertainty is larger, by $n\Delta\lambda$. Thus, if S/N is given for a unit $\Delta\lambda$, $\Delta W_\lambda(1\ \sigma) = \sigma(W) = n\ \Delta\lambda/n^{1/2}$ (S/N) = $\Delta\lambda/n^{1/2}$/(S/N). This equation applies strictly to the case of weak-line detection limits. When used as an uncertainty on a strong line, the equation gives a conservative value, since S should be calculated for each pixel and S is reduced in the pixels at the bottom of strong lines. However, the improvement derived from an exact calculation is usually not realized in fact, because the additional uncertainty in drawing the condinuum becomes relatively more important as lines become stronger.

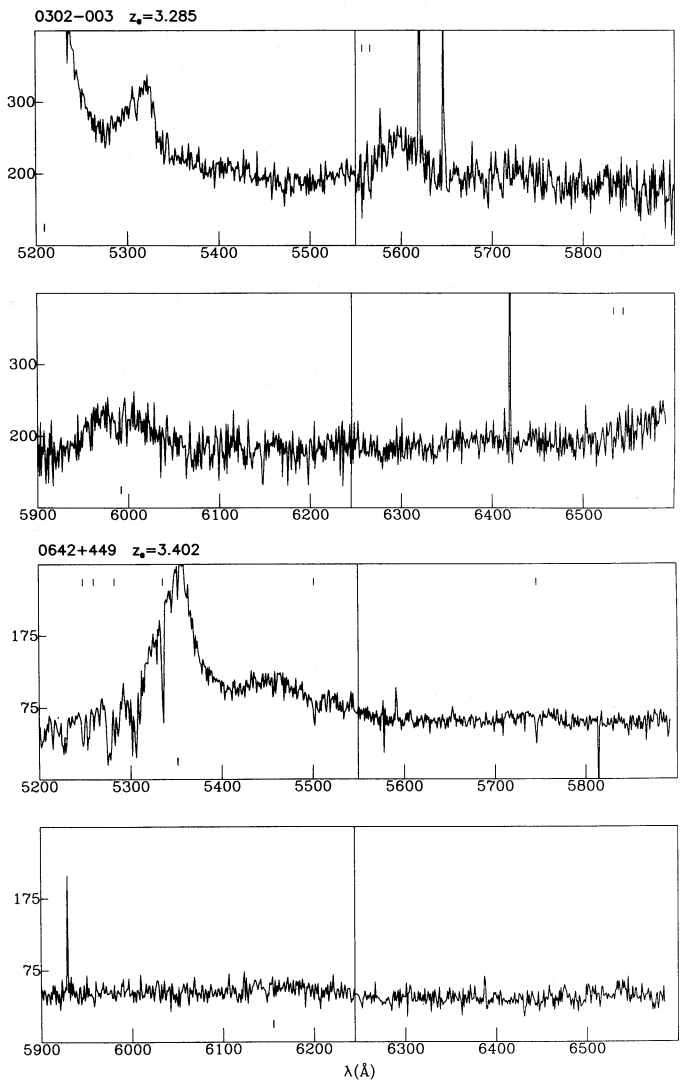

FIG. 1—*Continued*

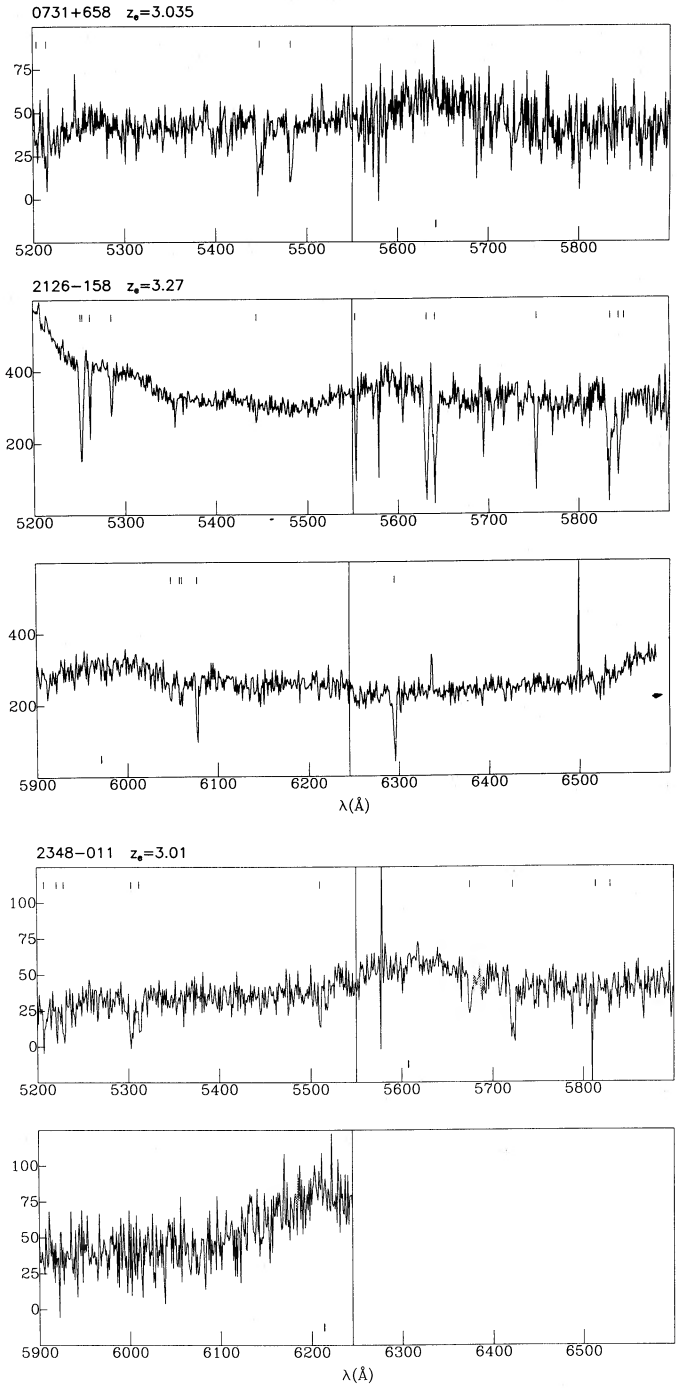

FIG. 1—*Continued*

Note that σ includes only the uncertainty in the observed equivalent width due to the uncertainty in the observed flux, which is the major source of error. The lines are listed in Table 2, along with their equivalent widths in angstroms and their identifications. The line list of Morton, York, and Jenkins (1988) was used for identifications. In some cases, an observed line could have been identified with two different lines belonging to different redshift systems, in which case the more likely identification is given in the table. The other identification is commented upon. Identification with the weaker (lower oscillator strength) of the multiple lines of an ion was rejected if the stronger line failed to appear, or if the equivalent width ratio of multiple lines of a given ion was significantly different from their expected values. In some cases, where a line which seemed to be crucial for identification of an absorption system appeared to be blended with other lines, we used Gaussian fitting to deblend the feature. In some cases, a line was obliterated by what appeared to be a bad pixel or a cosmic ray. Such cases, if crucial to the identification of an atom or ion, are commented upon, while the rest were left out of the line lists. We also compiled a list of lines with $5\,\sigma \geq W_{\rm obs} \geq 3\,\sigma$, and tried to identify them using the redshift systems defined by the lines with $W_\lambda > 5\,\sigma$, mainly to study ionization effects in well-established systems.

In order to classify absorption systems according to criteria based on the ionization level, it is very useful to know whether or not a particular ion is observable but undetected in a given redshift system. With this in mind, we have presented our data in a different fashion in Table 3. For each absorption system noted in Table 2, we give the rest equivalent width of absorption lines commonly observable in QSO spectra with $\lambda_{\rm rest}$

TABLE 2

ABSORPTION LINES

Number	λ_{obs}	W_{obs}	σ_W	S/N	ID	z_{abs}	W_r
Q 0014+81 (5200–6600 Å)							
1	5201.28[a]	2.33	0.05	26.82		...	...
2[b]	5204.88[a]	0.81	0.04	26.82		...	...
3	5218.09[a]	1.15	0.05	26.82		...	...
4	5225.4[a]	3.89	0.07	26.82		...	...
5[c]	5237.9[a]	1.54	0.06	26.82		...	...
6	5251.62[a]	8.44	0.09	26.82	H I (1215.6)	3.3199	1.954
7	5263.88[a]	0.78	0.06	26.82		...	...
8	5274.2[a]	1.12	0.07	26.82		...	...
9	5280.9[a]	0.39	0.04	26.82		...	...
10	5295.3[a]	1.21	0.06	26.82	Si IV (1393.7)	2.7993	0.318
11	5307.84[a]	1.39	0.05	26.82	C IV (1548.2)	2.4284	0.405
12	5317.9[a]	1.27	0.05	26.82	C IV (1550.8)	2.4292	0.370
13	5329.6[a]	0.66	0.07	26.82	Si IV (1402.7)	2.7993	0.174
14	5340.2[a]	0.55	0.04	26.82		...	...
15[d]	5356.8[a]	0.25	0.04	26.82		...	...
16	5378.6	0.2	0.04	26.82		...	...
17[e]	5407.19	0.41	0.05	26.82		...	...
18[f]	5442.01	0.49	0.06	26.82	S II (1259.5)	3.3207	0.113
19	5462.48	4.22	0.07	26.82	Fe II (2586.6)	1.1118	1.998
20	5478.25	0.26	0.04	26.82	Mn II (2593.5)	1.1123	0.123
21	5490.92	5.24	0.07	26.82	Fe II (2600.17)	1.1118	2.481
22	5882.17	2.098	0.13	14.26	C IV (1548.2)	2.7993	0.552
23	5891.74	2.27	0.13	14.26	C IV (1550.8)	2.7992	0.597
24	5905.41	6.81	0.16	14.06	Mg II (2796.3)	1.1118	3.335
25	5920.14	6.66	0.15	14.06	Mg II (2803.5)	1.1117	3.153
26	6024.88	1.07	0.11	14.06	Mg I (2852.1261)	1.1124	0.51
27	6541.8	0.78	0.13	9.7	C IV (1548.2)	3.2254	0.184
28	6552.77	0.68	0.13	9.7	C IV (1550.7)	3.2255	0.161
Q 0114−089 (5200–6600 Å)							
1	5221.28	0.47	0.09	12.27		...	...
2	5351.64	0.76	0.13	12.27		...	...
3	5365.55	0.58	0.11	12.27		...	...
4	5463.5	0.84	0.13	12.27		...	...
5	5478.1	0.81	0.1	12.27	C IV (1548.2)	2.5384	0.229
6	5487.4	0.45	0.08	12.27	C IV (1550.8)	2.5385	0.127
7	5584.1	0.56	0.08	15.01		...	...
8	5755.3	0.31	0.06	15.01		...	...
9	5891.36	0.80	0.11	15.01		...	...
10	5897.97	0.76	0.11	15.01		...	...
11	6354.2	3.05	0.16	13.27	C IV (1548.2)	3.1042	0.7431
12	6365.36	1.82	0.16	13.27	C IV (1550.8)	3.1046	0.4434
Q 0120+026 (5200–6600 Å)							
1	5315.4	0.89	0.15	12.58		...	...
2	5353.2	0.79	0.15	12.58	Mg II (2796.3)	0.9149	0.413
3	5364.5	1.21	0.16	12.58	Mg II (2803.5)	0.9140	0.63
4	5999.0	2.03	0.25	7.66		...	...
Q 0153+045 (5200–6200 Å)							
1	5263.04	2.551	0.17	11.71	C IV (1548.2)	2.3994	0.75
2	5271.99	2.556	0.16	11.71	C IV (1550.8)	2.3996	0.752
3	5300.77	1.753	0.14	11.71	C IV (1548.2)	2.4238	0.512
4	5309.13	1.642	0.18	11.71	C IV (1550.8)	2.4235	0.48
5	5465.43	1.028	0.11	11.71	C IV (1548.2)	2.5302	0.29
6	5469.37	0.551	0.09	11.71	Fe II (1608.4)	2.4004	0.16
7	5474.4	0.82	0.13	11.71	C IV (1550.8)	2.5301	0.23
8	5909.03	0.70	0.13	12.52		...	...
9	5932.71	2.09	0.15	12.52	C IV (1548.2)	2.832	0.545
10	5942.38	1.72	0.14	12.52	C IV (1550.8)	2.8319	0.449
11	6076.54	0.65	0.12	12.52		...	...
12	6153.55	0.43	0.07	17.2		...	...
Q 0302−003 (5200–6600 Å)							
1	5472.06	0.303	0.06	16.88		...	...
2	5557.14	0.59	0.08	13.8	C IV (1548.2)	2.5894	0.164
3	5565.97	0.79	0.13	10.69	C IV (1550.8)	2.5891	0.22

TABLE 2—*Continued*

Number	λ_{obs}	W_{obs}	σ_W	S/N	ID	z_{abs}	W_r
4	5710.3	0.86	0.17	10.69		...	...
5	5890.75	0.82	0.14	10.69		...	...
6[g]	6147.19	1.106	0.16	8.51	C IV (1550.8)	2.9639	0.279
7	6532.94	0.72	0.13	12.88	C IV (1548.2)	3.2197	0.171
8	6543.39	0.64	0.12	12.88	C IV (1550.8)	3.2194	0.152
Q 0642+449 (5200–6600 Å)							
1	5203.34[a]	1.81	0.15	9.24		...	...
2	5214.93[a]	1.467	0.14	9.24		...	...
3	5227.96[a]	4.121	0.21	9.24		...	...
4	5248.05[a]	2.363	0.17	9.24	Ni II (1741.5)	2.0134	0.784
5	5253.72[a]	2.213	0.17	9.24		...	...
6	5260.18[a]	0.92	0.18	9.24	Si II (1526.7)	2.4455	0.26
7	5276.37[a]	6.031	0.22	9.24		...	...
8	5282.7[a]	1.56	0.14	9.24	Ni II (1751.9)	2.0154	0.517
9	5286.4[a]	1.35	0.14	9.24		...	...
10	5304.4[a]	3.97	0.19	9.24		...	...
11	5310.1[a]	1.29	0.12	9.24		...	...
12	5335.6[a]	2.12	0.18	13.06	C IV (1548.2)	2.4463	0.615
13	5501.3	0.85	0.14	9.24	C IV (1334.6)	3.1220	0.206
14	5746.1	1.16	0.19	7.14	Si IV (1393.7)	3.1228	0.281
15	5896.2	1.46	0.27	7.14		...	...
16	5957.4	1.61	0.3	4.82	Si IV (1402.7)	3.2469	0.379
Q 0731+653 (5200–5900 Å)							
1	5204.15	1.705	0.31	5.3	C IV (1548.2)	2.3614	0.507
2[h]	5214.73	2.57	0.27	5.3	C IV (1550.8)	2.3627	0.764
3	5397.94	2.25	0.36	5.3		...	...
4	5447.96	5.07	0.39	5.3	Si IV (1393.7)	2.9088	1.297
5	5481.82	3.42	0.36	5.3	Si IV (1402.7)	2.9078	0.875
PKS 2126−158 (5200–6600 Å)							
1	5208.84	0.26	0.045	25.87		...	...
2	5252.51	2.76	0.07	24.29		...	...
2a	5251.83	1.88	0.05	24.29	Si IV (1393.7)	2.7681	0.499
2b	5253.89	1.01	0.05	24.29	C IV (1548.2)	2.3935	0.297
3	5262.09	0.92	0.06	24.29	C IV (1550.8)	2.3932	0.271
4	5285.29	0.75	0.05	24.29	Si IV (1402.8)	2.7677	0.199
5	5354.84	0.65	0.07	23.11		...	...
6[i]	5444.43	0.31	0.05	23.11	Si IV (1393.7)	2.9063	0.079
7	5553.05	1.37	0.05	23.11	Si II (1526.7)	2.6375	0.377
8	5631.92	3.91	0.19	9.93	C IV (1548.2)	2.6377	1.074
9	5641.29	2.83	0.16	9.93	C IV (1550.8)	2.6377	0.778
10	5695.13	0.77	0.11	9.93		...	...
11	5752.83	1.9	0.14	9.93	Si II (1526.7)	2.7680	0.504
12	5834.68	3.94	0.18	9.93	C IV (1548.2)	2.7687	1.046
13	5844.05	2.4	0.18	9.93	C IV (1550.8)	2.7685	0.636
14	5849.9	0.71	0.13	9.93	Fe II (1608.4)	2.6369	0.196
15	6048.61	0.84	0.13	12.35	C IV (1548.2)	2.9069	0.215
16	6059.65	0.2	0.13	12.35		...	...
16a	6058.39	0.58	0.09	12.35	C IV (1550.8)	2.9067	0.149
16b	6060.77	0.58	0.09	12.35	Fe II (1608.4)	2.7682	0.154
17	6077.32	1.59	0.1	12.35	Al II (1670.8)	2.6374	0.436
18	6211.64	0.56	0.1	12.35		...	...
19	6224.57	0.64	0.1	12.35		...	...
20	6295.21	2.67	0.6	13.9	Al II (1670.8)	2.7678	0.708
21	6521.09	0.79	0.13	13.9		...	...
Q 02348−011 (5200–6200 Å)							
1	5207.83	2.498	0.34	4.62	Mg II (2796.3)	0.8629	1.341
2	5221.74	1.308	0.23	4.62	Mg II (2803.5)	0.8631	0.702
3	5229.61	2.803	0.31	4.62	Si II (1526.7)	2.4254	0.818
4	5303.41	5.049	0.41	4.62	C IV (1548.2)	2.4255	1.474
5[j]	5312.32	3.96	0.44	4.62	C IV (1550.8)	2.4257	1.156
6	5510.27	1.768	0.27	4.62	Fe II (1608.4)	2.4259	0.516
7	5675.31	2.03	0.31	5.59	C I (1656.9)	2.4252	0.59
8	5722.92	4.92	0.36	5.59	Al II (1670.8)	2.4252	1.436
9	5813.95	1.509	0.28	5.59	Mg II (2796.3)	1.0791	0.726
10	5830.28	1.705	0.28	5.59	Mg II (2803.5)	1.0796	0.82

between 1216 and 1750 Å. In case the line has not been observed, we give a 2 σ upper limit. In some cases the line could be detected with 3 $\sigma > W_{obs} > 2\ \sigma$, and, in such cases, the observed value is given in Table 3. We also indicate whether or not a line at the given redshift was in the region observed for that QSO. Finally, we list the status of the absorption system, which we classify as certain (C), if (1) the absorption system contains at least one of the C IV, Mg II, or Si IV doublets with an appropriate equivalent width ratio, (2) each line of the doublet has $W_{obs} > 5\ \sigma$, and (3) the doublets are on the long-wavelength side of the Lyα emission. Other categories are probable (Pr) and possible (Po) in order of decreasing certainty. The reasons for such classifications are noted in footnotes to Table 3. Absorption systems based on 3 σ identifications are also included in Table 3.

For 2348−011, a system at $z_a = 2.598$ was reported by Smith, Cohen, and Bradley (1986), based on Lyα absorption, but we could not detect the corresponding C IV doublet lines at 3 σ level. However, lines at 5586.01 and 5596.4 Å corresponding to C IV at a redshift of 2.608 are present at the 2 σ level.

In Table 4, we have listed all the certain C IV absorption systems along with their rest equivalent widths. Also included are the relative velocities (βc) of the absorption systems with respect to the QSO. We define homogeneous samples for studying the statistical properties of the absorption systems. All systems in Table 4 form the sample S. Systems having a rest equivalent width of $\geq$0.3 Å for each member of the C IV doublet form the homogeneous sample S1, while systems in S1 which have $\beta > 0.015$ form sample S2, which presumably contains only the intervening systems as discussed in the next section.

III. PROPERTIES OF THE C IV ABSORBERS

a) *Distribution in Relative Velocity with Respect to the QSOs*

It is generally believed that the absorption systems, in the spectra of the QSOs without troughed systems,[5] having a relative velocity of $\lesssim$5000 km s^{-1} with respect to the QSO, are associated with the QSO or its environment (FWPSMC). These might arise, for instance, in clouds associated with rich clusters of galaxies containing the QSO. This suggestion was first elaborated on by Weymann *et al.* (1979), who observed an excess of absorption systems within a few thousand kilometers per second of a QSO sample. Such an excess was not observed by Young, Sargent, and Boksenberg (1982; hereafter YSB), but was confirmed by new observations of the Weymann *et al.* (1979) sample by FWSPSMC. They suggested that the difference with the YSB results probably occurs as a result of the difference in radio properties of the QSOs in the two samples, the associated systems being more common in the radio-loud QSOs with steep spectra.

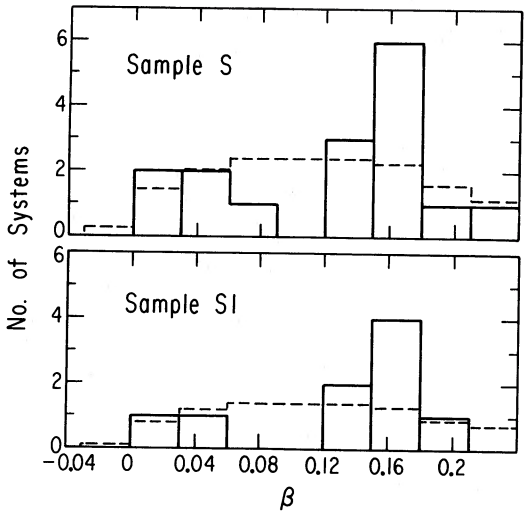

FIG. 2.—*Top*: histogram of system occurrence as a function of apparent ejection velocity (β) in units of the speed of light. Dashed line is the expected curve assuming no correlation of absorbers with the QSO. Solid line is for the actual data. Solid curve is for the sample S of Table 4 (all 5 σ detections of C IV doublets). *Bottom*: same as above, but for sample S1, the subset of sample S with $W_\lambda > 0.3$ Å in each member of the doublet.

In order to verify this result, we studied the distribution in β for our samples S and S1 to see if any excess in number of absorbers arises between $\beta = 0$ and $\beta = 0.04$. Over the small range in $z_{emission}$ in our sample (2.99–3.41), any absorbers found at $z_{abs} < z_{em}$ also cover a small range in z. A uniform distribution of absorbers with z, say with $dM/dz \propto (1+z)^\gamma$, $\gamma = 0$–2, where M is the number of components and $\gamma \sim 0.5$–1 for no evolution in volume density of absorbers, will have $dM/dz \sim$ constant (to 20%) and $dM/d\beta \sim$ constant. In each QSO, some range of β is covered, but the range in β is different for each object. Thus, a given range β_2–β_1 is covered in only a fraction of the objects. The number of absorbers in a given β range is the total number of absorbers observed times the relative coverage of that range. This expected distribution is plotted as a dashed line in Figure 2, while the actual distribution is plotted as a solid line. Results for samples S and S1 are shown. (For example, for sample S, $\beta = 0.05$ to $\beta = 0.15$ was observed in all objects, while only some objects were observed at $\beta = 0$ to $\beta = 0.05$ and $\beta = 0.15$ to $\beta = 0.24$).

[5] That is, the QSOs with wide P Cygni profiles, called broad absorption line QSOs, or BALs.

TABLE 2—*Footnotes*

[a] Shortward of Lyα emission, hence possibly blended with the Lyα forest.
[b] This line coincides with Ni^+ λ1370.1 at $z = 2.7993$, but Ni^+ λ1454.8 should be 400–800 mÅ and is definitely absent.
[c] This line coincides with Mg^+ λ1239.9, $z = 3.2254$, but the other member of the doublet cannot be confirmed because of confusion.
[d] Corresponds to Mg^+ λ1239.9 at $z = 3.3203$, but the other component of the doublet is absent.
[e] With $\lambda_{obs} = 5442.01$ Å (row 18), this could be a Si IV doublet, $z = 2.88$.
[f] S^+ λ1250.58, 1253.8 are present at the 3 σ level.
[g] C^{+++} λ1548 is weak ($< 5\ \sigma$).
[h] Blended with C^+ λ1334.53 at $z = 2.9083$, causing the large equivalent width.
[i] Other component of the doublet, present at 5480 Å but is $< 3\ \sigma$, probably due to bad night-sky subtraction.
[j] Mg λ2852 for $z_a = 0.8630$ blended with this line.

TABLE 3

ABSORPTION SYSTEMS[a]

z_a	Si III λ1206.5	Si IV λ1393.75	Si IV λ1402.77	Si II λ1526.7	C IV λ1548.2	C IV λ1550.77	Fe II λ1608.45	Al II λ1670.8	Ni II λ1741.55	Other Identifications with W_0	Status	Comments
0014+81												
1.1119	...	...	...	...	...	...	...	...	...	Fe II (2586.6) 1.998 Fe II (2600.2) 2.481 Mg II (2796.3) 3.225 Mg II (2803.5) 3.153 Mg I (2852.1) 0.51	C	1
2.4288	...	...	...	bl	0.405	0.37	<0.015	<0.027	<0.028		Pr	2
2.7993	...	0.318	0.174	<0.025	0.552	0.597	<0.025	<0.036	...		C	
2.8795	...	0.106	≤0.126	≤0.0432	0.043	<0.024	<0.024	<0.036	...		Po	3
3.2254	...	bl	bl	<0.033	0.184	0.161	...	...	...		C	
3.3203	<0.012	0.086	0.036	...	...	...	...	...	...	H I (1215.6) 1.954 S II (150.6) 0.046 S II (1253.8) 0.048 S II (1259.5) ≤0.113	C	1
0114−089												
2.5384	...	...	...	0.093	0.299	0.127	<0.025	<0.035	<0.035		C	
2.6544	...	...	...	<0.024	0.145	0.143	<0.024	<0.034	bl	C I (1560.3) 0.07	Pr	3
3.1044	...	0.056	<0.022	<0.025	0.743	0.443	...	...	...		C	
0120+026												
0.9144	...	...	...	...	...	...	...	...	...	Mg II (2795.5) 0.413 Mg II (2802.7) 0.63 Mg I (2852.1) 0.198	Pr	1
0153+045												
2.3998	...	...	...	...	0.75	0.75	0.16	<0.036	<0.032		C	
2.4237	...	...	...	<0.034	0.512	0.48	<0.034	<0.035	<0.031		C	
2.5301	...	...	...	<0.033	0.29	0.23	<0.034	<0.034	<0.03		C	
2.8319	...	<0.03	≤0.101	<0.031	0.545	0.449	...	...	...		C	
0302−003												
2.5892	...	...	...	0.089	0.164	0.22	<0.034	≤0.22	<0.045		C	
2.6887	...	...	...	0.062	0.233	0.192	0.057	<0.034	<0.034		Pr	3
2.9638	..	<0.079	<0.12	<0.16	0.273	0.279	<0.1	...	...		Pr	3
3.2195	...	<0.029	<0.037	<0.025	0.171	0.152	...	...	...		C	
0642+449												
2.0144	...	...	...	...	...	...	...	...	0.784	Ni II (1751.9) 0.517	Po	1
2.4459	...	...	...	0.26	0.615	0.086	0.12	0.155	0.17	Ni II (1709.0) 0.15	Po	2
2.491	...	...	...	...	<0.042	<0.042	<0.054	<0.054	0.19		Po	3
2.911	...	<0.037	0.07	<0.07	0.16	0.37	0.136	<0.086	...		Pr	3
2.971	...	0.106	<0.047	0.33	0.42	0.11	...	...	...		Pr	3, 4
3.1224	...	0.28	0.09	<0.083	<0.083	<0.083	...	...	...	C II (1334.6) 0.21	Pr	
3.191	...	<0.045	0.091	<0.081	0.25	0.20	...	...	...		Pr	3
3.246	...	<0.066	0.379	0.105	0.29	0.12	...	...	...		Pr	3

TABLE 3—*Continued*

z_a	Si III λ1206.5	Si IV λ1393.75	Si IV λ1402.77	Si II λ1526.7	C IV λ1548.2	C IV λ1550.77	Fe II λ1608.45	Al II λ1670.8	Ni II λ1741.55	Other Identifications with W_0	Status	Comments
						0014+81						
2.3620.....	...	...	...	...	0.507	≤0.764	<0.092	0.22	0.286		C	
2.9083.....	...	1.297	0.875	...	...	...	...	...	...	S I (1425.03) 0.33 C II (1334.53) bl	C	1
						2126+58						
2.3933.....	...	...	...	...	0.297	0.271	0.068	0.106	0.035		C	
2.6374.....	...	...	...	0.377	1.074	0.778	0.196	0.436	...		C	5
2.7681.....	...	0.499	0.199	0.504	1.046	0.636	0.154	0.708	<0.025	C I (1560.3) 0.11	C	
2.9066.....	...	0.079	...	0.046	0.215	0.149	<0.024	0.056	...	S I (1425.03) 0.14	C	6
						2348−011						
0.8629.....	...	...	...	...	...	...	...	...	...	Mg II (2796.35) 1.34 Mg II (2803.53) 0.702 Mg I (2852.1)	C	1
1.0793.....	...	...	...	...	...	...	...	...	...	Mg II (2796.35) 0.73 Mg II (2803.53) 0.82 Mg I (2852.1) 0.13	C	1
2.4255.....	...	...	...	0.818	1.474	1.156	0.516	1.436	≤0.388	C I (1656.9) 0.59	C	

[a] Three ellipsis dots indicate the predicted wavelength is outside the range of observations. Upper limits are 2 σ. A " < " sign is used when the line coincides with some other (probably weak) line as noted in Table 2, or the line falls in a neighboring unidentified line. The symbol " bl " indicates that the line is blended with a strong line ($W_r > 0.2$) which is occasionally unidentified.

COMMENTS.—(1) C IV is out of range; hence, the system is not part of our C IV sample. (2) C IV identified is in the Lyα forest and hence, could be misidentified or too strong. (3) Identification based on 3 σ lines, identifiable on the plots but not tabulated in Table 2. (4) Fe^+ λ1608 destroyed by bad pixel or cosmic ray. (5) Ni^+ λ1741 destroyed by bad pixel or cosmic ray. (6) Si^{+++} λ1402.8 destroyed by bad pixel or cosmic ray.

TABLE 3B

DETECTION RATES, GIVEN C IV, FOR SI IV AND VARIOUS FIRST IONS

	Si IV		All First Ions		Mg II		Si II		Fe II		Al II		Ni II	
Δz	P	O	P	O	P	O	P	O	P	O	P	O	P	O
1.1–1.9[a].....	...	...	31	11	31	11	...	...	...	...	...	...	...	...
1.0–2.0[b].....	5	2	13	3	...	...	13	2	13	0	9	2	...	...
2.4–3.2[c].....	5	3	15	4	...	...	12	4	12	2	12	3	9	0

[a] Caulet 1989.
[b] FWPSMC. Detections are 5 σ.
[c] This paper. Detections are 5 σ. One Si IV system contains no C IV ($z = 3.1224$, Q 0642+449).

TABLE 4

C IV ABSORPTION SYSTEMS ($z_{min} = 2.3587$)

QSO	z_{abs}	β	W_r $\lambda = 1548.2$	W_r $\lambda = 1550.8$	Sample
0014+81	2.7993	0.148	0.552	0.597	S[a], S1[b], S2[c]
	3.2254	0.0427	0.184	0.161	S
Q 0114−089	2.5384	0.1604	0.229	0.127	S
	3.1044	0.0134	0.743	0.443	S, S1
Q 0153+045	2.3998	0.1587	0.75	0.752	S, S1, S2, S3[d]
	2.4237	0.1519	0.512	0.48	S, S1, S2
	2.5301	0.1218	0.29	0.23	S
	2.8319	0.0404	0.545	0.449	S, S1, S2
Q 0302−003	2.5892	0.175	0.164	0.22	S
	3.2195	0.0154	0.171	0.152	S
Q 0731+653	2.3620	0.1805	0.507	≤0.764	S, S1, S2
Pks 2126−158	2.3933	0.2258	0.297	0.271	S
	2.6374	0.159	1.074	0.778	S, S1, S2, S3
	2.7681	0.1244	1.046	0.636	S, S1, S2, S3
	2.9066	0.0887	0.215	0.149	S
Q 2348−011	2.4255	0.1533	1.474	1.156	S, S1, S2, S3

[a] Sample S includes all systems in the table, chosen to include systems with both members of the C IV doublet detected at the 5 σ level, longward of Lyα emission from the background QSO.
[b] Sample S1 is the subset of S with both members of the doublet stronger than $W_\lambda = 0.3$ Å.
[c] Sample S2 is the subset of S1 with apparent ejection velocity, β, greater than $0.015c$; these are generally regarded as intervening systems, where as the subset of sample S2 with $\beta < 0.015c$ may include material at high velocity originating in the QSO itself.
[d] Sample S3 is the subset of S2 with $W_\lambda > 0.6$ Å.

The number of systems with $\beta < 0.04$ is completely consistent with the intervening hypothesis (i.e., no excess is found in the observed sample). There is a dearth of systems at $\beta \sim 0.1$ and an excess at $\beta = 0.16$. We performed χ^2 tests to determine whether the expected and observed distributions are drawn from the same sample and found that for samples S and S1 (Table 4) the probabilities that the differences in the observed and expected distributions would occur by chance are 0.177 and 0.208, respectively. The excess observed near $\beta \sim 0.16$ is related to the excess at $z = 2$–2.5 discussed later.

Thus, the data are consistent with all of our sample of C IV systems arising in the intervening galaxies. Out of our nine QSOs, only three are known radio sources and only one of them (0642+449) has a spectral index >0.7 (Veron-Cetty, and Veron 1987). For this last QSO, the observations do not cover the region $\beta < 0.015$. We conclude that our data are not in conflict with the conclusion of FWPSMC. That is, the sample does not include the type of radio sources that seem to make the sample of FWPSMC differ from that of YSB. For our sample, the systems with $\beta < 0.04$ do not demand special treatment; that is, they may be counted as intervening systems for statistical purposes.

b) *Equivalent Width Distribution*

The equivalent width distribution of absorption systems in samples excluding systems with $\beta < 0.015$ was studied. (We note that even a chance intervening system near a QSO may have ionization and, hence, equivalent width properties affected in a special way by the QSO radiation field or by jets from the AGN. For this comparison, we therefore ignore the systems with low β.) The functional form was taken to be that assumed by, for instance, Tytler (1986):

$$m(W) = (m_*/W_*)e^{-W/W^*},$$

$m(W)$ being the number of absorption systems per unit redshift interval per unit rest equivalent width interval around W, the rest equivalent width of the 1548 Å line of the C IV doublet. Using the maximum likelihood method to fit the observed distribution, we find

$$m_* = 4.67 \pm 2.17,$$

$$W_* = 0.2896 \pm 0.0611,$$

at the average redshift of $\bar{z}_a = 2.63$. The fit is shown in Figure 3. The probability that the observed distribution differs from the

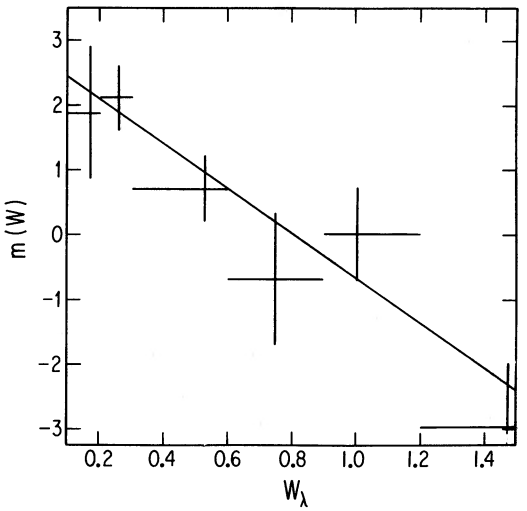

FIG. 3.—Equivalent width distribution for the sample S with systems $\beta < 0.015$ removed. Solid-line fit is described in the text. Vertical lines are 1 σ errors, while horizontal lines indicate bin width.

fitted distribution by chance is as large as 0.5. The values of m_* and W_* differ significantly from the values 1.76 and 0.88, respectively, for Mg II systems (Lanzetta. Turnshek, and Wolf 1987; hereafter LTW). They also differ from the values 3.55 and 0.5 (see LTW) obtained by YSB for C IV systems. The results of LTW and YSB are for low-redshift systems with $\bar{z} \sim 1.7$. The equivalent width distribution of the C IV systems thus seems to be a function of redshift, consistent with there being relatively more weak systems as z increases.

c) *Ionization Properties of the Absorbers*

The well-documented QSO absorbers at $z < 2.5$ have a wide range of ionization states present. No adequate classification exists yet, nor can it until accurate column densities are available for a large number of systems. Since saturation is evident in many observed doublets, such determinations must be based on observations of better resolving power ($\lambda/\Delta\lambda > 30{,}000$; Bechtold, Green, and York 1987).

However, some general comments can be made based only on equivalent widths. To aid in intercomparing systems, Table 3A is laid out so detection of the main species to which our wavelength coverage is sensitive is evident for all observed systems. Entries with values are measured W_λ's, upper limits are so noted, and unobservable lines are left blank. The symbol "bl" means the line is blended.

The rest wavelength region 1300–1750 Å generally scanned in surveys of this type contains Si IV, C IV, and a number of first ions (Si II, Al II, Fe II, and Ni II). To compare, crudely, the ionization state of the absorbers at different redshifts, we tabulate in Table 3B the incidence of detection of these species given the presence of C IV. The result of Caulet (1989), who searched for Mg II in known C IV systems, is listed first. For each species, "P" denotes that the species was scanned in a relevant system and "O" denotes that it was seen. Results from FWPSMC and from this paper are given in the last two lines.

Thus, among 5 σ detections, there is a slight trend toward more frequent occurrence of first ions at higher redshift. Presumably because Mg II has stronger lines than the other first ions and is less depleted in interstellar gas, Mg II is the first ion most often seen. If the observed trend is real, we expect Mg II to be quite common in systems at $z > 2.0$ ($\lambda > 8400$ Å).

We note that if the whole of Table 3 is considered, including detections at the 3 σ or 4 σ level, first ions occur in 50% of the systems, about twice the detection rate noted in Table 3B. From the FWPSMC comments, their table seems to include second ions of lower statistical significance when they belong with significant C IV systems. It is remarkable that one additional Si II line appears at a lower significance level, while no extra lines of Al II, Fe II, or Si IV appear. There is thus the suggestion that first ions are seen more often at $z > 2.5$ than at $z < 2.5$, but deeper surveys are needed to establish this point.

d) *Number Density and Evolution of the Absorbers*

The main objectives of the present survey were to determine the number density of the absorbers at high z and to obtain information regarding the evolution of the properties of these absorbers. The number of absorption systems per unit redshift per line of sight (M) is given by

$$\frac{dM}{dz} = \frac{c}{H_0} n_0 \sigma_0 \frac{(1+z)^{\alpha+1}}{(1+2q_0 z)^{0.5}} .$$

Here n_0 and σ_0 are the present values of the number density and cross section of the absorbers, repectively. A value $\alpha > 0$ implies evolution in $n\sigma$ in the sense that σ increases and/or n increases as one looks back to earlier times. $\alpha < 0$ implies absorbers are being created, or growing, as z decreases. For $q_0 = 0$ or $\frac{1}{2}$, this can be written as

$$\frac{dM}{dz} = \left.\frac{dM}{dz}\right|_0 (1+z)^\gamma ,$$

where $\gamma = \alpha + 1$ for $q_0 = 0$, and $\gamma = \alpha - 0.5$ for $q_0 = \frac{1}{2}$. Thus, dM/dz should increase linearly with $1 + z$ (for $q_0 = 0$), or as $(1+z)^{0.5}$ (for $q_0 = \frac{1}{2}$) for no evolution. The value of dM/dz should then increase by a factor of $\sqrt{2}(q_0 = \frac{1}{2})$ to $2(q_0 = 0)$ between $z = 1$ and $z = 3$.

In order to study evolution over as large a redshift range as possible, we combined our data with that of FWPSMC. They have used the same spectral resolution of 1 Å and have similar S/N. For statistical analysis, the sample of QSOs must ideally be unbiased; i.e., it should not have been chosen based on the prior knowledge of the absorption systems. Both our sample and that of FWPSMC satisfy this criterion. FWPSMC have counted as one all the redshift systems within 2000 km s^{-1} of each other, to account for possible correlation between C IV doublets. Sargent (1988) considers the possibility that systems less than 600 km s^{-1} apart are part of the same galaxy, as suggested by York *et al.* (1986). Most known systems have $\Delta v \lesssim 300$ km s^{-1} (Yanny and York 1989), a value we adopt here. Choosing $\Delta v = 200$ km s^{-1} or 1000 km s^{-1} does not affect our conclusions. We extend our sample S by including all the systems in FWPSMC with $W_{\rm obs} > 5\ \sigma$, and extend our sample S2 by including systems with $W_{\rm obs} > 5\ \sigma$, $W_r > 0.3$ Å for each line of the C IV doublet and $\beta > 0.015$ from the FWPSMC sample. We also construct a sample S3 containing only those systems from sample S2 which have $W_r > 0.6$ Å for each line of the C IV doublet. The redshift range observed for each QSO in FWPSMC for systems satisfying criteria of samples S, S1, and S2 was calculated by scaling their 4 σ equivalent width limits as a function of wavelength (Foltz, private communication) to obtain 5 σ equivalent width limits as a function of wavelength. Another large and unbiased sample available in the literature is that of YSB. We have not included their sample in our study for two reasons. First, their resolution is lower than that of both FWPSMC and our sample, and, second, 5 σ equivalent width limits as a function of wavelength were not available for their sample; it was therefore not possible to check the uniformity of criteria for such limits for the whole sample, nor would it have been possible to determine the number of lines of sight observed for the extended sample S4 (defined below).

For each of the samples S, S2, and S3 we divide the observed redshift interval into five bins with $\Delta z = 0.5$ each. In Table 5, we give the number of observed lines of sight (MLS), number of absorption systems observed (NAS), dM/dz, and the average redshift for each bin for the three samples. To consider the effects of including weaker lines, we have also constructed a sample S4 which contains absorption systems having $W_{\rm obs} > 4\ \sigma$, $W_r > 0.2$ Å for each line of the C IV doublet, and $\beta > 0.015$. Results for this sample are also included in Table 5. The results are plotted in Figure 4 for samples S2, S3, and S4.

It is immediately evident that dM/dz is not monotonic with z. For all samples S, S2, S3, and S4, the value dM/dz peaks at $z = 2$–2.5. (Recall sample S includes all 5 σ systems; S2 contains systems with W_λ for each C IV line > 0.3 Å and $\beta > 0.015$,

TABLE 5

NUMBER DENSITY OF C IV ABSORBERS AS A FUNCTION OF REDSHIFT

	S				S2				S3				S4			
Bin Size	NLS	NAS	dM/dz	$\bar{z}_a$	NLS	NAS	dM/dz	$\bar{z}_a$	NLS	NAS	dM/dz	$\bar{z}_a$	NLS	NAS	dM/dz	$\bar{z}_a$
1.0–1.5[a]	14.1	8	1.1	1.491	12.7	5	0.8	1.4	13.1	2	0.3	1.442	12.4	7	1.1	1.384
1.5–2.0[a]	20.6	29	2.8	1.732	11.6	6	1.0	1.703	11.6	1	0.2	1.675	11.6	7	1.2	1.676
2.0–2.5[b]	3.3	5	3.0	2.401	2.1	4	3.8	2.403	2.1	2	1.9	2.413	1.6	3	3.8	2.406
2.5–3.0[b]	8.6	8	1.9	2.700	8.4	4	1.0	2.759	8.3	2	0.5	2.703	6.9	6	1.7	2.755
3.0–3.5[b]	3.1	3	2.0	3.183	2.5	0	...	...	2.5	0	...	...	2.0	0	...	...

[a] All systems from FWPSMC.
[b] All systems from this paper.

to eliminate associated systems; S3 includes lines >0.6 Å; S4 allows 4 σ systems and $W_\lambda > 0.2$ Å). Although the samples are small, the peak persists as the samples are redefined. The most dramatic difference between the samples occurs when $\beta < 0.015$ systems are eliminated (S to S2). In fact, dM/dz for associated systems ($\beta < 0.015$), in the five bins of Table 5, is 0.3, 1.8, 0.8, 1.9, and $\lesssim 2.0$, showing no peaking. The value $n\sigma$ for intervening C IV systems appears to peak in the range $z = 2$–2.5.[6]

Various claims exist in the literature for evidence of evolving values $n\sigma$, from $\gamma = 2 \pm 1$ (Bergeron and Boisse 1984) to $\gamma = -1.4 \pm 0.4$ (Sargent 1988). We have attempted to test these extremes for consistency with our sample (see lines in Fig. 4). Either model can be excluded from fitting our sample at the 5 σ level. The peak at $z = 2$–2.5 is too high to be accommodated by any value of γ. The apparent excess arises from a high detection rate in the most poorly observed redshift range of the sample that we can define ($z = 2.0$–2.5; see Table 5). The validity of such a high detection rate (one) system each time a QSO is observed over the full range 2.0–2.5) should be relatively easy to confirm, if valid.

[6] Note, from our earlier discussion in § III*a*, that the systems at $\beta < 0.015$, $z > 3$ may be intervening, not associated, in which case the value dM/dz at $z > 3$ for associated systems in the last bin of Table 5 is $\lesssim 1$, not $\lesssim 2$. Absorbers near luminous QSOs may be selectively destroyed, a possibility to be investigated with a different sample.

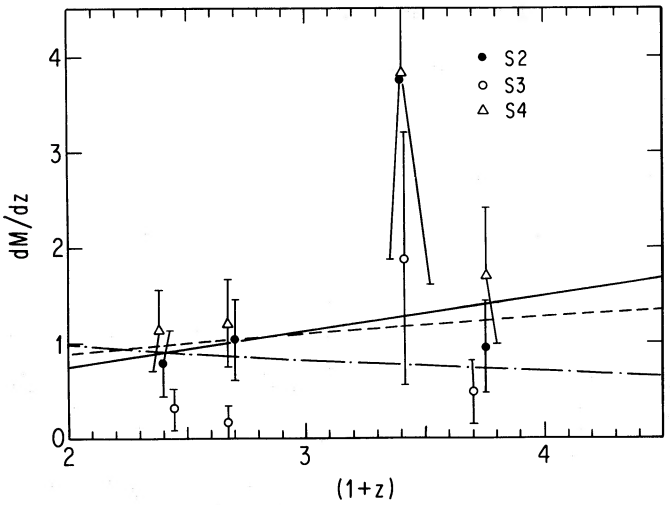

FIG. 4.—Number density of C IV absorbers as a function of redshift. Curves for $(1 + z)^\gamma$ for $\gamma = -0.5$, and 1.0 with arbitrary normalization are plotted for comparison.

YSB observed lines of sight covering the redshift range 2–2.5, but the coverage is heavily biased toward the lower part of the range. Therefore, it is not clear whether their finding no systems meeting the criteria of our sample S2 in the equivalent of three lines of sight (short segments of many QSOs) contradicts our result of an excess in the bin or not. (Our segments are biased toward the high-z end of the bin). Such statistical questions can only be settled with a larger sample. (We have checked for a large-scale structure effect, but both the YSB sample and our sample are spread in the sky and overlap significantly, so the differences are not caused by structure on the largest scales. Structure on scales of less than 30° at $z \sim 2.3$ could account for the differences, assuming we observed an excess of line-rich directions and YSB a dearth of such directions).

Figure 4 includes lines with power-law exponents -0.5, 0.5, and 1, normalized to roughly coincide with sample S2 (5 σ detections in C IV, $W_\lambda > 0.3$ Å, $\beta > 0.015$) near $z \sim 1.5$. It is evident that future examination of the evolution of $n\sigma$ must be based on larger samples. To separate creation or growth of absorbers at low z [$dM/dz < dM/dz|_0(1 + z)^{0.5}$, say] from destruction or contraction at low z [$dM/dz > dM/dz|_0(1 + z)^{0.5}$] at the 3 σ level requires observation of about 35 QSOs in each bin $\Delta z = 0.5$ at $z > 2$, chosen so the objects for each bin satisfy the constraint that the search bin lies between Lyα emission and 8500 km s$^-$ shortward of C IV emission. Such a sample of optically selected QSOs with $z_{em} \sim 2.5$–2.7 would be sufficient to establish whether the dM/dz is monotonic with z or has structure near $z \sim 2$–2.5.

IV. CONCLUSIONS

A magnitude-limited sample (incomplete, due to observing constraints) of $z > 3$ QSOs between 21^h and 8^h ($\delta > -10°$) has been observed at 1 Å resolution to search for high-z C IV doublets ($z = 2.3$–3.2). Thirty-five possible QSO absorption line systems are identified, 22 of which were not previously known. Twenty-one of the 35 systems are certain. Sixteen represent cases where both members of the C IV doublet are detected at the 5 σ level.

Comparisons of the various absorber properties are made between our sample and various low-z samples. While the small sample makes firm conclusions difficult to draw, three trends in our data deserve further study. All apply to the intervening absorbers ($\beta > 0.015$).

First, the distribution of C IV equivalent widths, while functionally consistent with studies at low z, indicates weak C IV lines are relatively more numerous. Caulet (1988) has suggested the opposite effect for Mg II, which seems to have relatively more weak lines at $z < 1$ than at $z > 1$.

Second, the frequency of occurrence of Si^+ and Si^{+++} in conjunction with C IV, is comparable at high z and at low z. A slight trend toward more frequent occurrence of low-ionization lines at high z may be present. This conclusion could be modified as uniform samples with consistent detection limits become available ($W_{rest} \lesssim 20$ mÅ).

Finally, the comoving density of absorbers decreases, on average, beyond $z = 2.5$, in spite of the increase from $z \sim 0.5$ to 2 found by previous authors. Since dividing an already small sample into several redshift bins necessarily complicates the problem in terms of statistics, a larger sample is obviously needed. Further studies of the number evolution of the absorvers may provide new information on the collapse and the morphology of forming galaxies. Confirmation could signal the detection of the accretion ($z > 2.5$), and eventually settling to equilibrium configurations ($z < 2$) of galaxies.

After this paper was submitted, we learned of the similar but larger study of Sargent, Boksenberg, and Steidel 1988 (hereafter SBS). Whereas the samples are of comparable size at $z > 2.5$ (they sample 18 lines of sight of $\Delta z = 0.5$ between $z = 2.5$ and $z = 3.0$; we sample eight), their coverage at $z = 2.5$ is much better. From Figure 4 of their paper, they cover $\Delta z = 0.5$ in that range for 30 sight lines compared to 3.3 in Table 5. This is just the sample size referred to earlier as necessary to establish the presence of the peak near $z = 2.4$ in Figure 4 of the present paper; the peak is not confirmed in SBS's Figure 7, which uses the sample definition most comparable to our own. The general structure (rise from $z = 0$ to $z \sim 2$, and fall at $z > 2.5$) is in fact confirmed (Sargent, Steidel, and Boksenberg 1988; hereafter SSB).

The existence of the peak in our sample is certain (that is, the systems defining it are real, and the normalization to a given redshift range is straightforward). It would then appear that one can pick a sample which has a line density 2–3 times higher in a bin $\Delta z = 0.5$ than that appearing in a larger sample. This may constitute evidence for large-scale structure, the possible existence of which is separately discussed by SSB. Our sample for the $\Delta z = 2$–2.5 bin is weighted toward the high-z end, so the effective width is $\Delta z < 0.5$. Structure on scales $\Delta z \sim 0.2$ is apparent in Figure 4 of SSB, which is washed out in binning by $\Delta z = 0.5$. Such structure may account for our large peak as well. Quite coherent structure on scales $\Delta z \sim 0.06$ and angles $\lesssim 1°$ is found in the histogram of galaxy redshifts out to $z \sim 0.5$ (Broadhurst, Ellis, and Shanks 1988; Koo and Kron 1987), and it is not yet known what the angular scale of coherence may be. The effect noted here and that noted in the galaxy distribution may be related.

However, there may still be some problems with definition of individual systems (SSB find higher dM/dz at $z = 1$–2, $W > 0.3$ Å than do FWPSMC.)

Several qualitative results appear to agree between our study and that of SSB. First, the data are consistent with a rise in dN/dz from $z = 0$ to $z > 1$ and a drop in dN/dz at $z > 2$. From the data of SBS and SSB, the peak is near $z \sim 2$ and broad; from our data it is sharper and at $z = 2$ to 2.5. Second, a sharp drop at $z > 2.7$ is evident in both data sets. Third, our result that C IV lines are weaker at high z is consistent with the increasing doublet ratio at high z found by SBS. Finally, there is evidence for a change in gross ionization properties between samples at $z < 2$ and $z > 2$, a point not made explicitly by SBS but apparent in their tabulated data. The trend is in the sense that relatively more detected C IV systems have Fe II, Si II, and Al II at $z > 2.0$ than at $z < 2.0$.

We are grateful to the Director of Kitt Peak National Observatory for allocation of time for this project, and to the excellent assistance of the staff at KPNO. D. G. Y. acknowledges support from the Farr Fund and from the Dean's Discretionary Fund at the University of Chicago. P. K. is grateful to Brian Yanny for introducing her to the IRAF packages and for help in presenting the spectra.

REFERENCES

Bechtold, J., Green, R. F., and York, D. G. 1987, *Ap. J.*, **312**, 50.
Bergeron, J. 1988, in *QSO Absorption Lines: Probing the Universe*, ed. J. C. Blades, D. Turnshek, and C. Norman (Cambridge: Cambridge University Press), pp. 127–146.
Bergeron, J., and Boisse, P. 1984, *Astr. Ap.*, **133**, 374.
Broadhurst, T. J., Ellis, R. S., and Shanks, T. 1988, *M.N.R.A.S.*, **235**, 827.
Caulet, A. 1989, *Ap. J.*, **340**, 90.
Foltz, C. B., Weymann, R. J., Peterson, B. M., Sun, L., Malkan, M. A., and Chaffee, F. H., Jr. 1986, *Ap. J.*, **307**, 504.
Hewitt, A., and Burbidge, G. 1987, *Ap. J. Suppl.*, **63**, 1.
Khare-Joshi, P., and Perry, J. J. 1982, *M.N.R.A.S.*, **199**, 785.
Koo, D., and Kron, R. 1987, in *IAU Symposium 124, Observational Cosmology*, ed. A. Hewitt, G. Burbidge, and L.-Z. Fang (Dordrecht: Reidel), pp. 383–388.
Lanzetta, K. M., Turnshek, D. A., and Wolfe, A. M. 1987, *Ap. J.*, **322**, 739.
Morton, D. C., York, D. G., and Jenkins, E. B. 1988, *Ap. J.*, **333**, 1037.
Sargent, W. L. W. 1988, in *QSO Absorption Lines: Probing the Universe*, ed. J. C. Blades, D. Turnshek, and C. Norman (Cambridge: Cambridge University Press), pp. 1–15.
Sargent, W. L. W., Boksenberg, A., and Steidel, C. C. 1988, *Ap. J. Suppl.*, **68**, 539 (SBS).
Sargent, W. L. W., Steidel, C. D., and Boksenberg, A. 1988, *Ap. J.*, **334**, 22 (SSB).
Smith, H. E., Cohen, R. D., and Bradley, S. E. 1986, *Ap. J.*, **310**, 583.
Tytler, D. 1987, *Ap. J.*, **321**, 1986.
Veron-Cetty, M. D., and Veron, P. 1987, ESO Sci. Rept. No. 5.
Weymann, R. J., Williams, R. E., Peterson, B. M., and Turnshek, D. A. 1979, *Ap. J.*, **234**, 33.
Yanny, B., and York, D. G. 1990, *Pub. A.S.P.*, in preparation.
York, D. G., Caulet, A., Rybski, P., Gallagher, J., Blades, J. C., Morton, D. C., and Wamsteker, W. 1990, *Ap. J.*, in press.
York, D. G., Dopita, M., Green, R. F., and Bechtold, J. 1986, *Ap. J.*, **311**, 610.
Young, P., Sargent, W. L. W., and Boksenberg, A. 1982, *Ap. J.*, **252**, 10.

RICHARD F. GREEN: Kitt Peak National Observatory, 950 North Cherry Street, P.O. Box 26732, Tucson, AZ 85726

PUSHPA KHARE: Physics Department, Ukal University, Vani Vihar, Bhubaneswar 751004, India

DONALD G. YORK: AAC002, 5640 South Ellis Avenue, Chicago, IL 60637